AIAA Paper 91-2955

Utilization of Simulation Tools in the HL-20 Conceptual Design Process

E. Bruce Jackson
W. A. Ragsdale
Richard W. Powell

NASA Langley Research Center
Hampton, Virginia

Presented at the AIAA Flight Simulation Technologies Conference
New Orleans, Louisiana
12-14 August 1991

UTILIZATION OF SIMULATION TOOLS IN THE HL-20 CONCEPTUAL DESIGN PROCESS

E. Bruce Jackson*
NASA Langley Research Center
Hampton, Virginia 23665

W. A. Ragsdale†
UNISYS Corporation, Hampton, Virginia
Hampton, Virginia 23665

Richard W. Powell**
NASA Langley Research Center
Hampton, Virginia 23665

Abstract

The NASA Langley Research Center (LaRC) is in the conceptual design stage of the Personnel Launch System (PLS). The passenger-carrying portion of the PLS system is a 20,000 pound lifting body vehicle, known as the HL-20.

Previous programs have demonstrated the controllability and "landability" of unpowered lifting body vehicles with low lift-to-drag (L/D) ratios; however, one of the early lifting body designs demonstrated an instability in the lateral-directional axes.

To evaluate the flight characteristics of the HL-20 design, a real-time simulation of the HL-20 lifting body vehicle has been developed at LaRC. The simulation model is being used to validate the HL-20 concept, identify opportunities for improving the design of the vehicle, and to develop preliminary designs for both automatic and manual control systems.

This paper describes the development of the real-time simulation, including development of manual and automatic flight control laws. Key results from use of this simulation are described, including identification of improved landing gear geometry, a requirement for aerodynamic improvements, and increased confidence in the improved HL-20 design.

Introduction

The NASA Langley Research Center (LaRC) is in the conceptual design stage of the Personnel Launch System (PLS). The Personnel Launch System consists of a booster and a lifting body, coupled with adapter hardware, to allow for vertical launch to orbit, followed by an unpowered horizontal landing at the end of the mission. The passenger-carrying portion of the PLS system is a 20,000 pound lifting body vehicle, known as the HL-20. The HL-20 lifting body design features a crew compartment large enough to house two crewmembers and eight passengers (figure 1).

The HL-20 is intended to serve as an Assured Crew Return Vehicle for Space Station Freedom, as a "space taxi" to ferry astronauts to and from the space station, and as a vehicle to perform other low earth orbit missions that do not require significant payload capability (satellite repair, free-flyer platform maintenance, and orbital rescue are examples). Other design features include a detachable one-piece heat shield, easy access to vehicle subsystems via lift-off panels for maintenance, and rapid mission turn-around following a horizontal landing. The cross-range capability is sufficient to allow a daylight landing at one of five designated landing sites on any orbit.

Previous programs[1,2,3] have demonstrated the controllability and "landability" of lifting-body vehicles with low lift-to-drag (L/D) ratios; however, an early lifting-body demonstrated an instability in the lateral-directional axes.[4]

Early identification of problems in the flight characteristics of the HL-20 should result in less expensive solutions than if the problems are discovered later in the development program.

In order to identify deficiencies in the HL-20 concept, simulation studies of the flight characteristics were developed, and several candidate control laws were designed. These simulation studies included a nonreal-time simulation, used for launch, orbit, and re-entry and guidance to final approach to the landing facility, and a real-time simulation used to study the low supersonic and subsonic phases of the re-entry, including approach and landing on a simulated runway.

An earlier paper described the nonreal-time simulation study and results.[5] This paper will describe the real-time simulation setup, the HL-20 real-time simulation model, and several candidate flight control system designs, as well as preliminary results from these real-time studies.

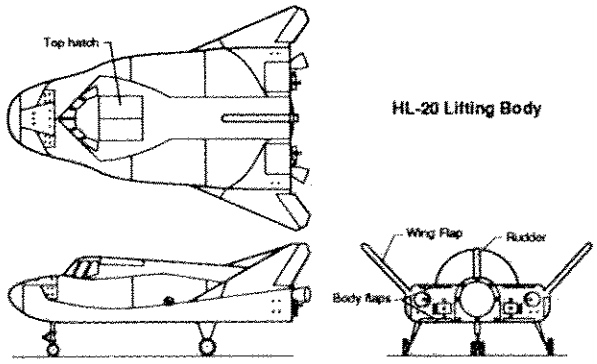

Figure 1. - HL-20 Three View Drawing

*Aerospace Engineer, Aircraft Guidance and Controls Branch, Guidance and Control Division, Member AIAA

**Aerospace Engineer, Vehicle Analysis Branch, Space Systems Division, Member AIAA

†Staff Engineer, Senior Member AIAA

Nomenclature

D	Drag, lbs
g	Gravitational constant (approx. 32.2 ft/sec^2)
L	Lift, lbs
N_Z	Normal acceleration, g's
$\dot{V}$	Rate of change of velocity, ft/sec^2
V_{rel}	Velocity relative to earth, ft/sec
γ	Flight Path Angle, degrees
$\dot{\gamma}$	Flight Path Angle rate, degrees/second

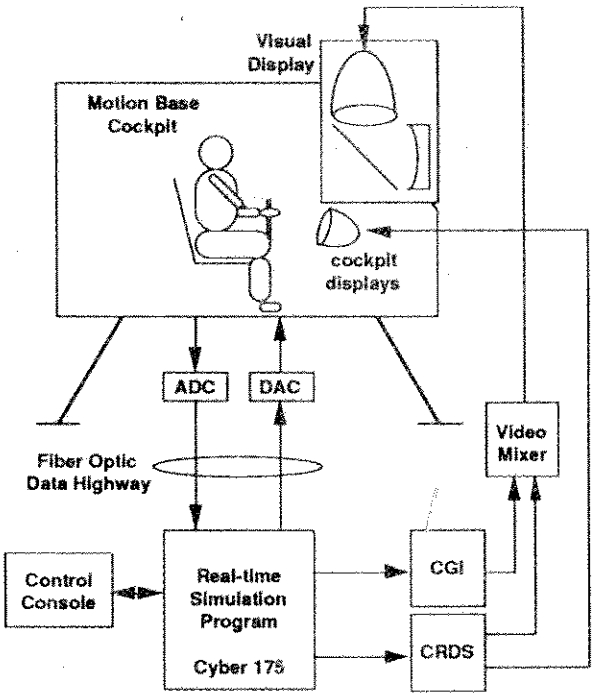

Figure 2. - Real Time Simulation Schematic

Discussion

Real-time Simulation Set-up

To find out if the HL-20 concept had any serious deficiencies in performance or handling qualities during the approach and landing phase, a real-time simulation effort was undertaken. Using preliminary wind tunnel data, a subsonic aerodynamic model of the HL-20 was developed[6]. This aerodynamic model was combined with an atmosphere model, equations of motion, and preliminary control laws to yield a six-degree-of-freedom approach and landing simulation capability. This model was then installed on the Transport Systems Research Vehicle fixed-base cockpit at LaRC, and used to conduct preliminary flying qualities and landing studies[7]. Follow-on studies have been performed using the Visual Motion Simulator cockpit, with an expanded aerodynamic model valid to Mach 4.

The host computer used in these studies was a Control Data Corporation CYBER-175, running at a frame rate of 33.3 Hz. Simulation peripheral equipment in both cases included an Evans and Sutherland CT-6 computer image

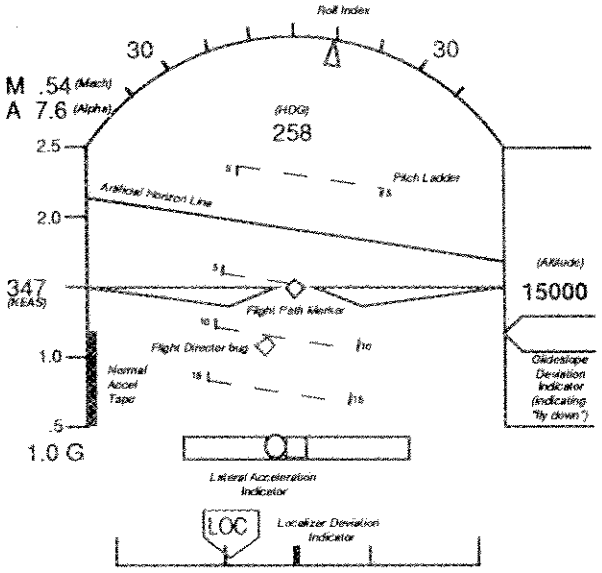

Figure 3. - Electronic Attitude Display Indicator Schematic

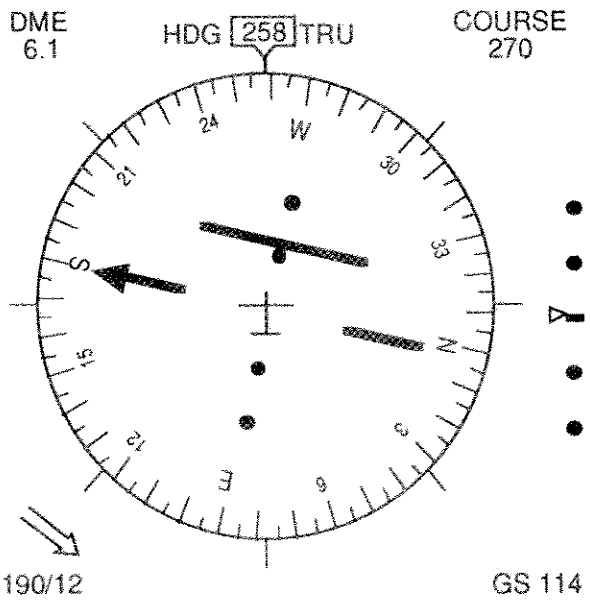

Figure 4. - Horizontal Situation Display Schematic

generator (CGI), and a McFadden side-arm controller. The heads-down display was provided by a Terabit Eagle graphics generator, known as the calligraphic/raster display system (CRDS). For further realism, a sound system provided generic wind noise and landing gear touchdown sounds. A diagram of the setup used in these simulations is shown in figure 2. Representations of the cockpit electronic attitude display indicator (EADI) and the horizontal situation display (HSD) are shown in figures 3 and 4.

A heads-up display (HUD) was provided, in later studies, by the CRDS. The HUD included flight director and velocity vector information, as well as airspeed, altitude, flight path reference markers and a preflare cue, in a manner similar to one of the declutter modes of the Shuttle Orbiter HUD. A typical HUD representation is shown in figure 5.

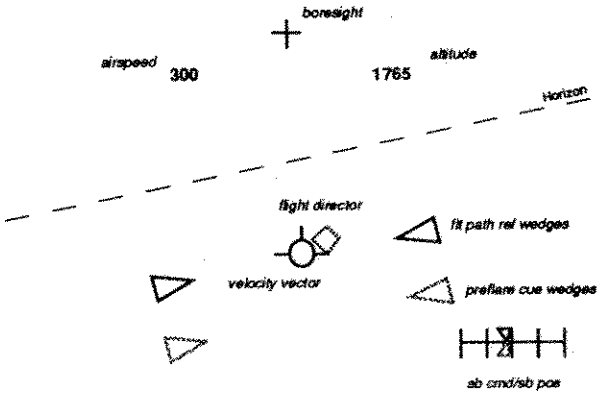

Figure 5. - Heads-Up Display schematic

A set of Precision Approach Path Indicator (PAPI) lights were displaced on the extended centerline of the runway to serve as the aimpoint for the outer glideslope. Unlike the Shuttle Landing Facility, however, no inner glideslope (ball-bar) was depicted. A typical view as seen by the pilot through the forward window while on approach to landing, including overlaid HUD symbology, is shown in figure 6.

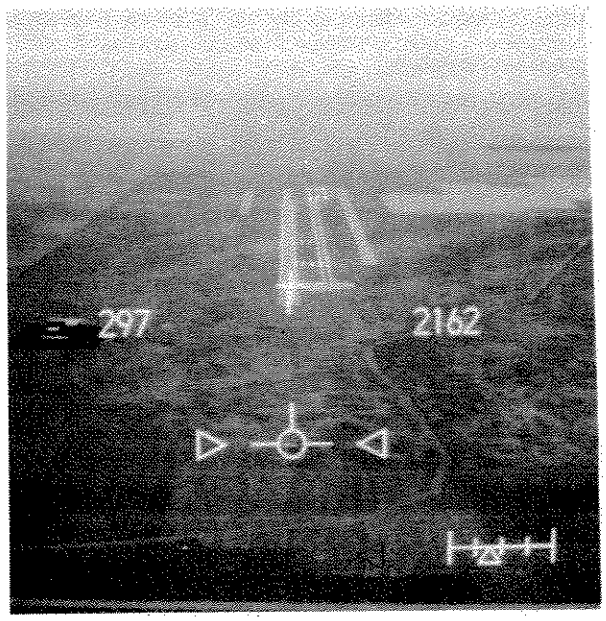

Figure 6. - Pilot's view approaching preflare height

Flight Control Systems

Several different flight control systems were designed to provide artificial stabilization and flight control of the vehicle in the subsonic regime. These control systems included a set of candidate manual control systems for use in the subsonic regime, and an automatic landing system. These control systems were developed using both real- and nonreal-time simulation facilities.

Baseline Control Laws

The initial control law, used in early studies, included a simple rate feedback system which provided increased damping in all three axes, and included an aileron-to-rudder interconnection to improve the coordination of turns (figure 7). It was later discovered that this interconnection

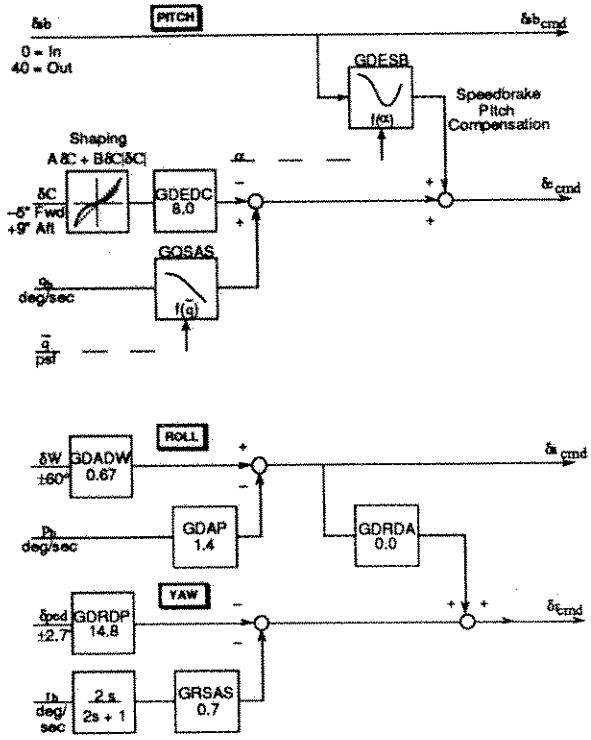

Figure 7. - Baseline Flight Controls

caused difficulties in performing uncoordinated maneuvers during crosswind landings and was removed with minimal impact on sideslip response in turns.

As shown in figure 7, the pilot's pitch input (delta column, or δC) passes through a shaping filter, then multiplied by a gain (GDEDC). The sign is then reversed to match elevator deflection sign convention (trailing edge down is positive). For stability, the aircraft pitch rate (q_b) is fed back at this point. A portion of the speedbrake command (δsb) is added to the result to remove pitch response from speedbrake deflection. The sum of these three signals is sent to the control surface mixer as δe_{cmd}.

The roll axis combines the pilot's roll input (delta wheel, or δW) with a roll rate feedback measurement (p_b) for stability. This signal is then sent to the control surface mixer as an "aileron" command (δa_{cmd}).

The pilot's rudder pedal position (δped) is summed with yaw rate feedback for stability. The yaw rate signal (r_b) is first sent through a washout filter to allow for steady turns. A portion of the aileron command is added to this signal when gain GDRDA is non-zero; simulator studies showed better crosswind landing capability when GDRDA was zero. The result is sent to the control surface mixer as δr_{cmd}.

In the course of piloted simulator evaluations of the HL-20, several modifications to the initial control system were made to make the flared, unpowered landing easier to accomplish. These improvements were made only to the pitch axis; the lateral/directional control laws remained unchanged. These "experimental" control laws are described below.

Experimental Control Laws - Justification

Landing a low-L/D vehicle, such as the HL-20, is very different from landing a conventional aircraft. The sink rate

on final approach is over 150 ft/sec at a speed of about 300 knots. This must be reduced to less than 5 ft/sec as the aircraft approaches the ground, and maintained at a low value until touchdown.

An unpowered aircraft in nearly level flight will decelerate at a rate given by:

$$\dot{V} = -\frac{g}{L/D} \qquad (1)$$

Thus, a vehicle with an L/D of 4.0 will decelerate at about 8 ft/sec^2, or about 5 knots per second. Dynamic pressure is proportional to velocity squared, and thus is rapidly decreasing. So, to maintain lift equal to weight, the angle of attack must be increased continuously. Furthermore, the low-aspect ratio of the HL-20 requires a greater increase in angle of attack than a conventional wing to effect a given change in lift. Also, the elevator trim angle will change significantly, since the touchdown speed is approximately 100 knots less than the approach speed, due to deceleration during the flare.

The result is that the landing maneuver in this vehicle requires a constantly increasing non-linear pitch rate.

The original baseline control system for this simulation consisted of a pitch rate feedback control law. This essentially generated an elevator command proportional to the difference between the pilot's stick input and the pitch rate of the aircraft. Although adequate for in-flight maneuvering, this system was somewhat difficult to land because it required ever increasing back-stick inputs during the landing flare.

An attempt was made to improve the system by adding an 'auto trim' feature. In this attempt, the existing elevator position was fed back through a first order filter and added to the existing elevator command. This resulted in a control law that would pitch at a rate proportional to stick deflection and hold a constant pitch attitude when the stick was released. This system was dubbed a 'Rate Command Attitude Hold' or RCAH control law.

Most aircraft are controlled and landed by reference to the pitch attitude. Pitch attitude is the parameter that can be observed most easily by the pilot. However, in the HL-20 pitch attitude is never constant during the landing flare, but must be increased at a non-constant rate and more rapidly at lower speeds. The RCAH system was unsatisfactory for landings and tended to induce oscillations.

The major aerodynamic forces during landing (lift and drag) are generated by the angle of attack. Although it cannot be directly observed by the pilot, angle of attack is an excellent control parameter for some flight modes. However, angle of attack must also be increased continuously at a non-constant rate in landing the HL-20.

The parameter that is actually being controlled in a landing is the flight path angle, or 'gamma', equivalent to the vertical direction of the velocity vector. The required gamma at any point in the landing is easily estimated. It is a constant value on the outer glide slope, and is roughly proportional to the altitude during the flare, reducing to zero at touchdown. If an aircraft can be designed to hold a given 'gamma command' it can be landed safely.

A pure 'gamma command' system is difficult to implement, however. A direct measurement of gamma itself is not easy to produce, and is sensitive to instrumentation errors and failures. It is also difficult to generate gamma commands with a control stick, as pilots generally expect a rate response from their inputs. It was found in the simulator that some pilots tended to get out of phase during rapid maneuvers with the gamma command system, resulting in a pitch oscillation.

A better approach than pure 'gamma command' is to feed back the rate of change of gamma, or 'gamma dot'. Such a system is more natural to pilots, and maintaining gamma dot equal to zero is equivalent to holding gamma at a constant value.

The most direct digital method for generating gamma dot would be to numerically differentiate gamma itself. This method is even more sensitive than 'gamma command' to numerical problems, instrumentation errors, wind gusts, and pilot induced oscillations.

Some of these difficulties can be alleviated by passing gamma through a washout filter. Mathematically, this is equivalent to calculating the derivative of gamma and then feeding it through a first-order lag. This method, dubbed the 'Gamma Washout' law, was the first experimental law evaluated in the HL-20 study. It resulted in the easiest and best landings by most pilots (see Simulator Results).

However, the Gamma Washout system still requires an accurate measurement of gamma itself. A second method was developed which estimates gamma dot without requiring any knowledge of gamma. In nearly level flight, the rate of change of gamma can be estimated from the following relationship:

$$\dot{\gamma} = 57.3\,\frac{g(N_Z - 1)}{V_{rel}} \qquad (2)$$

N_Z and V_{rel} are standard parameters that can be derived accurately from a number of possible sources. The combination of gamma dot, derived from N_Z, and pitch rate feedback, compared to the pilot's stick inputs, resulted in the 'NZQ' control law. This control law will pitch at a rate proportional to the pilot's stick deflections, and maintain one-G when the stick is released. Its performance is nearly the same as the Gamma Washout law. The only noticeable difference is that slight back pressure is required to maintain a constant sink rate as the ground is approached. This results in the NZQ law being less likely to produce 'ballooning' or pilot induced oscillations near touchdown.

It may be possible to improve the NZQ control law by additional filters, shapers, and turn coordination terms, but it appears to be acceptable in its simplest form.

Experimental Control Laws - Description

As shown in figure 8, the pilot's pitch stick input (δC) is first passed through a shaping function. The shaping function can be varied from a straight linear function to a pure quadratic ('square law') function, or anything between, depending on the 'square law ratio' (0 for a linear law, 1 for a quadratic law). A value of 0.6 was determined experimentally to have the most preferred characteristics.

The shaped column command is passed through a gain (GDQDC) to produce a pitch rate command. With the RCAH option there are no other active commands. In the Gamma Washout option, gamma is passed through a washout filter with a 1.0 sec time constant to produce an additional pitch rate command proportional to gamma dot. Likewise, in the NZQ option, gamma dot is estimated from N_Z and V_{rel} inputs (per equation above) and added to the pitch rate command signal. In either case a fixed gain, GDEGC, is used to control the amount of pitch rate required to maintain gamma dot approximately zero with no column inputs.

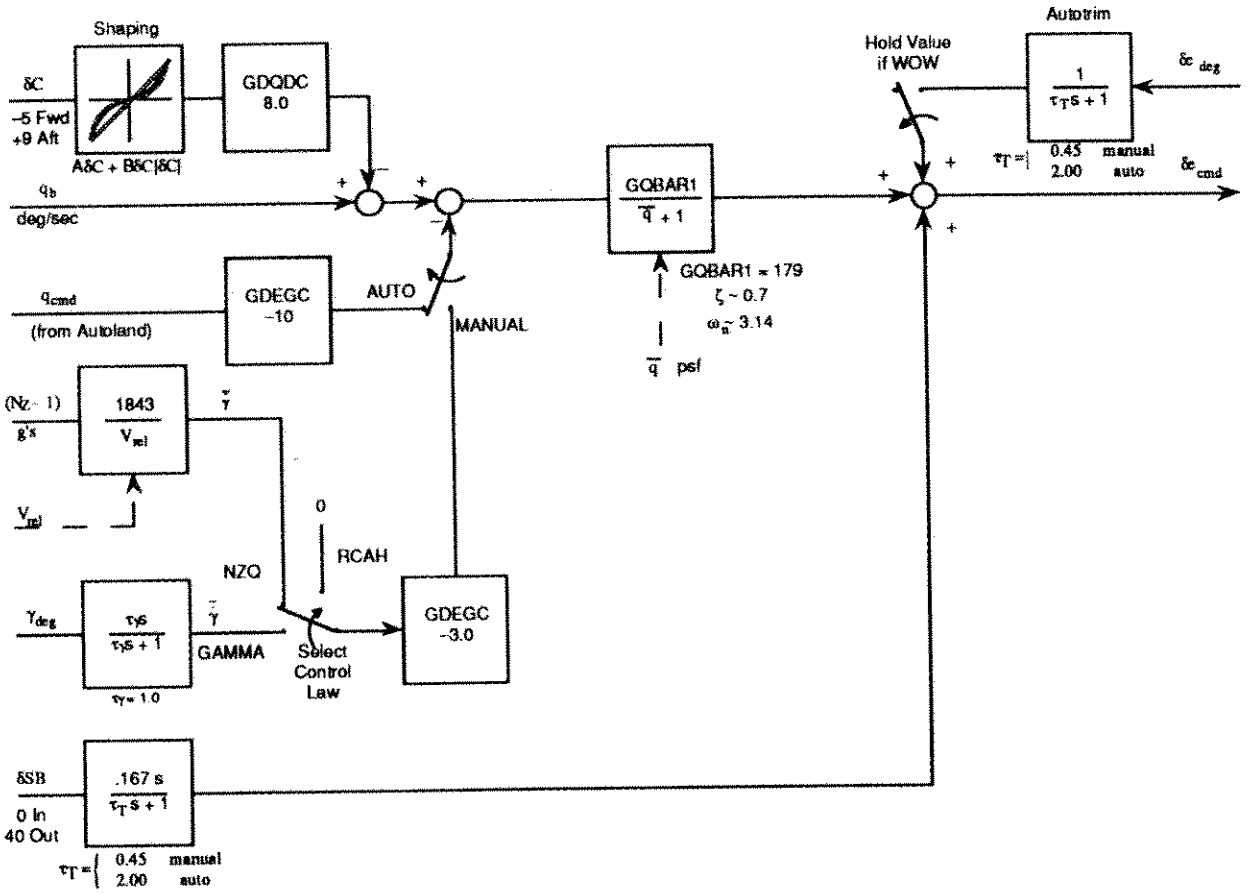

Figure 8. - Experimental Pitch Control Laws

If Autoland mode is engaged, a pitch rate commanded by the guidance program is added to the command signal. The pilot may make additional inputs during Autoland mode, without disengaging it.

The command signal is multiplied by a variable gain inversely proportional to dynamic pressure (Q-bar) to compensate for the variation in control effectiveness due to dynamic pressure. The gain (GQBAR1) is designed to produce a pitch rate step input response with a damping ratio of 0.7 and natural frequency of 3.14 rad/sec at 200 knots (the typical touchdown speed).

The elevator trim command ('auto trim') is determined by a lagged feedback of the present elevator deflection added to a speedbrake compensator. The speedbrake compensator consists of a gained washout of the speedbrake deflection, that drives the elevator trim whenever the speedbrake is in motion. The elevator feedback value is held constant at the value existing when 'weight-on-wheels' (WOW) is detected at main gear touchdown.

The total elevator command is the sum of the command input and the trim command. The elevator command is routed to the elevon actuators, which are simulated as first-order actuators with a time constant of 0.1 sec, rate limited to 200 degrees/second, and a deflection limit of 40° up or down.

Autoland Guidance & Control Laws

Figure 9 depicts the Autoland control laws used in the HL-20 simulation. These laws generate pitch rate and aileron deflection commands which are summed with other quantities in the inner loop pitch and roll stabilization programs.

Autoland was typically engaged and flown for the entire approach. The implementation allowed the pilot to make corrective inputs that were added to the autoland signal; this was not necessary as a rule, since the autoland, having a perfect "nav state" (i.e. navigation sensor and filter errors were not modeled), worked well. Disengagements of autoland and reversion to manual control were not attempted after an approach began.

The outputs of these autoland guidance laws are also used to drive a flight director on the EADI and on the HUD for the pilot's use, even when autoland was not engaged. The flight director depicts the difference between the state of the vehicle (flight path angle and bank angle) and the state commanded by the Autoland algorithm.

Vertical Steering

The pitch control law uses flight path angle as its primary reference. Gamma command is a good parameter to use for pitch guidance, since it is constant for most of the approach and is nearly zero at touchdown. By comparison, angle of attack or pitch commands must be varied as a function of airspeed and control deflections. Gamma command is also directly compatible with the Gamma Washout and NZQ control laws used for manual control in this simulation, and with the HUD velocity vector display which was used for out-the-window cues.

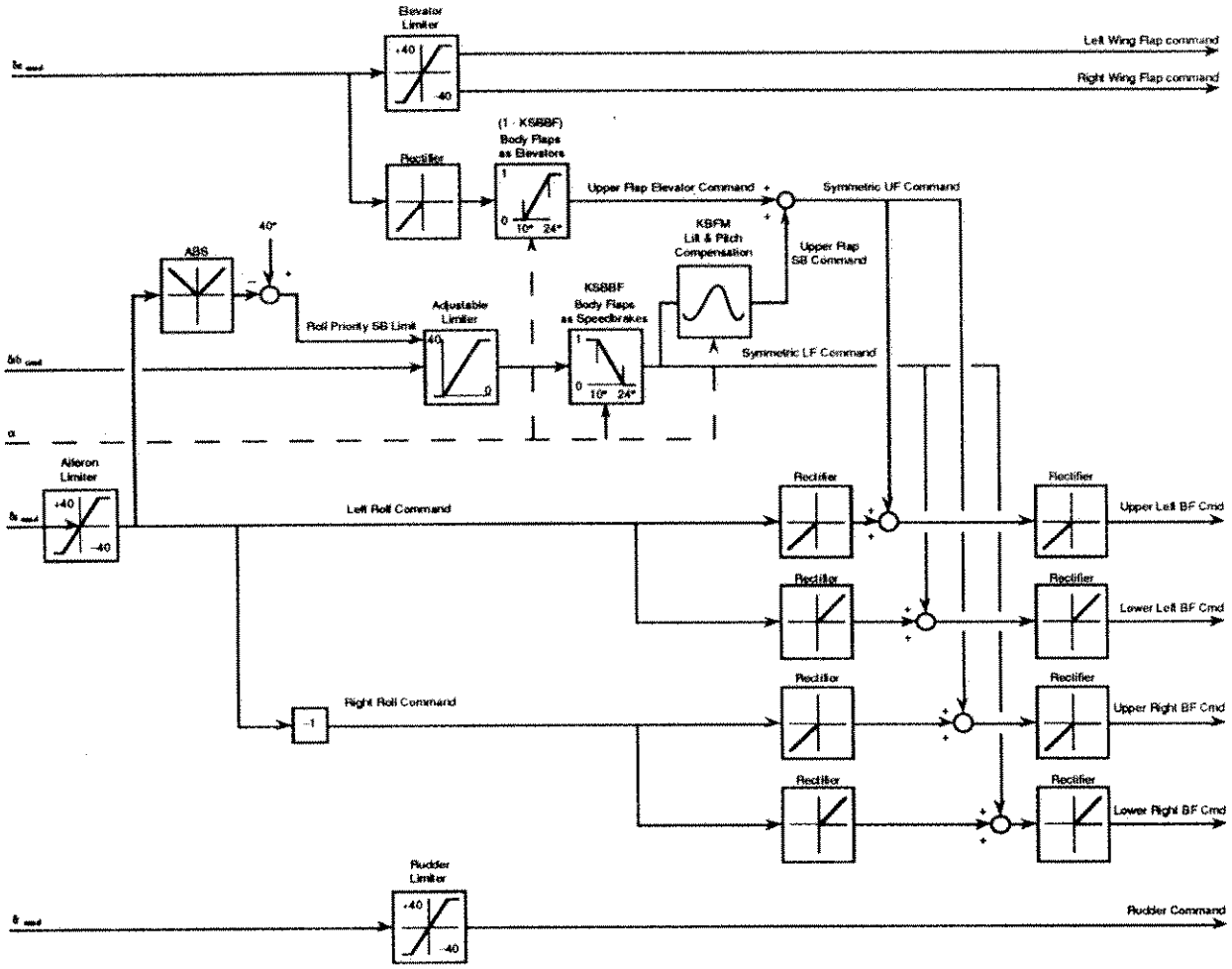

Figure 10. - Control Surface Mixing Laws

As shown in figure 9, the lateral displacement from centerline, Y_{RWY}, is multiplied by a gain to produce an centerline intercept angle command. This gain linearly increases below 5000 ft altitude to avoid unnecessary abrupt commands at higher altitudes, and still stay on the centerline as the runway is approached. The track angle command is the sum of the runway centerline heading, ψ_{RWY}, and the intercept angle command.

A track error is obtained by subtracting the actual ground track angle, ψ_{TRK}, from the commanded ground track angle. The resulting track error is resolved into ±180° and multiplied by a fixed gain to determine a roll angle command, which is limited to 40°.

The guidance aileron command is then obtained by multiplying the difference between the actual and commanded roll angles by a fixed gain. The aileron command is limited to 15° and sent to the roll flight control program, where it is summed with pilot inputs and roll stabilization commands. As in the longitudinal case, the pilot may make inputs which are added to the Autoland commands without disengaging Autoland.

Control surface mixer

The HL-20 conceptual design includes seven aerodynamic control surfaces, as shown in figure 1. These include an all-movable vertical fin, two wing flaps, and four body flaps - two located on the upper surface on the body and two located on the lower surface. These body flaps are only capable of deflections outward, away from the body. This control surface arrangement is similar to earlier lifting bodies (ref. 2,3,4).

The control laws described above yield commands for an "aileron", "elevator", "speedbrake", and "rudder". Since the HL-20 has an unconventional control arrangement, these commands are passed through a controls mixer that separates these four commands into seven separate control surface commands.

The same control mixing arrangement was used for all subsonic control system configurations and is shown in figure 10. The wing flaps were used symmetrically for pitch control, and, at higher angles of attack, the upper body flaps were used for additional pitch control. The body flaps were deployed simultaneously for speedbrake and asymmetrically for roll control. The rudder was used for yaw control.

The use of wing flaps for roll control was investigated, but they showed a significant amount of adverse yawing moment. While the vehicle would initially roll in the commanded direction, this adverse yawing moment would result in a yaw in the opposite direction. Since the HL-20 has a strong aerodynamic "dihedral" effect, the resulting sideslip caused the vehicle to eventually roll in the opposite direction, against the commanded roll. Using asymmetric

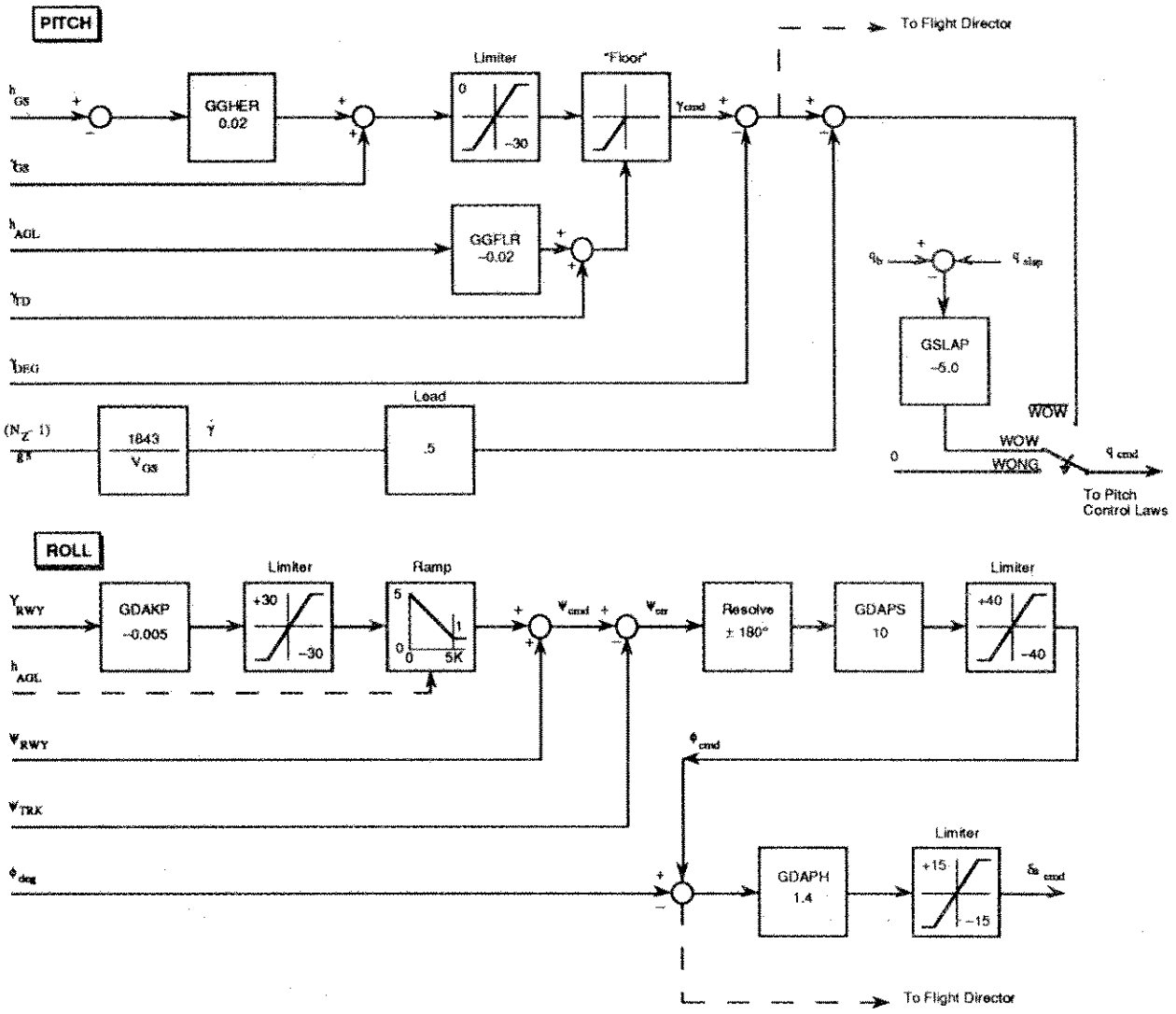

Figure 9. - Autoland Control Laws

Glideslope guidance consists of three segments--an outer glideslope with a fixed flight path angle of -17.0°, a 1.25 g pullup, and an inner glideslope of -1.0°. As shown in figure 9, the altitude of the aircraft is compared to the nominal glideslope altitude at the present downrange distance to produce an altitude error signal. The altitude error is multiplied by a fixed gain, and added to the nominal glideslope gamma to produce a preliminary gamma command.

The gamma command is then limited to avoid values that are either too steep (resulting in excessive airspeed and sink rate) or too shallow (resulting in a stall). The upper gamma command limit corresponds to flying at the maximum L/D condition until flare altitude is reached. Between flare and touchdown the upper limit is level flight, or zero gamma.

The gamma command lower limit is further limited by a 'floor' value proportional to altitude. If the aircraft is sinking at a rate that would impact the ground in a few seconds, the gamma command is reduced to initiate a pullup. At zero wheel altitude the floor value is equal to the desired gamma at touchdown, thus providing the final flare command.

Gamma rate is estimated from the vertical acceleration (N_Z) and earth relative velocity. To smooth performance, gamma is projected 0.5 sec ahead, by adding the present gamma plus 0.5 times gamma rate. The final pitch command sent to the inner loop is the difference between the gamma command and the projected gamma. A fixed gain in the flight control inner loop results in a pitch rate command, summed with other control inputs. The pilot may make inputs which are added to the Autoland command without disengaging Autoland.

After weight-on-wheels the Autoland law commands a 'slapdown' at 5 degrees/second, and after weight-on-nosegear (WONG) the Autoland commands are zeroed.

Lateral Steering

The lateral steering algorithm calculates aileron deflection commands to achieve a roll angle that maintains a ground track angle along the extended runway centerline (or 'localizer').

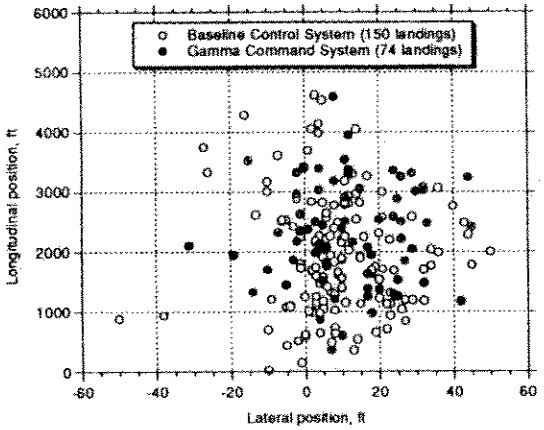

Figure 12. - Effect of improved longitudinal control system on landing dispersion; L/D ~ 3.2

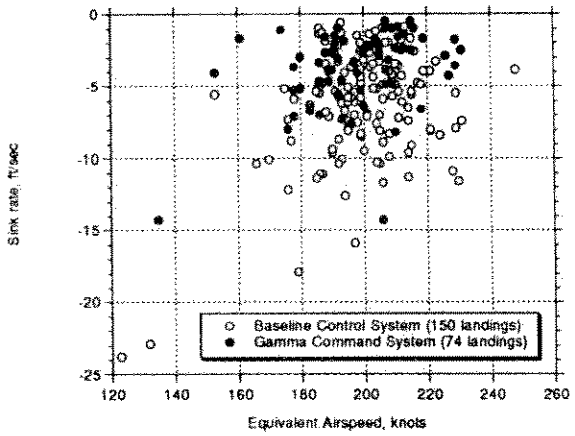

Figure 13. - Effect of improved longitudinal control system upon touchdown velocities; L/D ~ 3.2

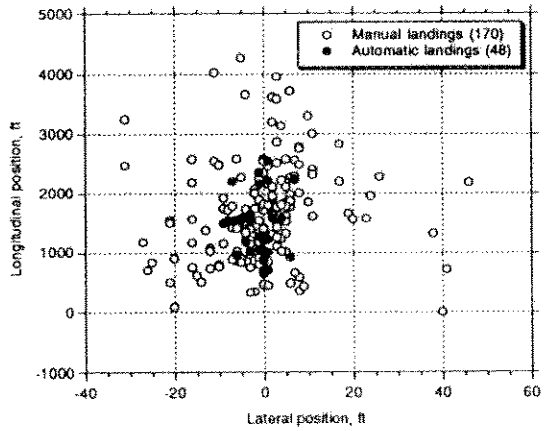

Figure 14. - Touchdown dispersion for manual and automatic landings in various wind and turbulence conditions; L/D ~ 4.3

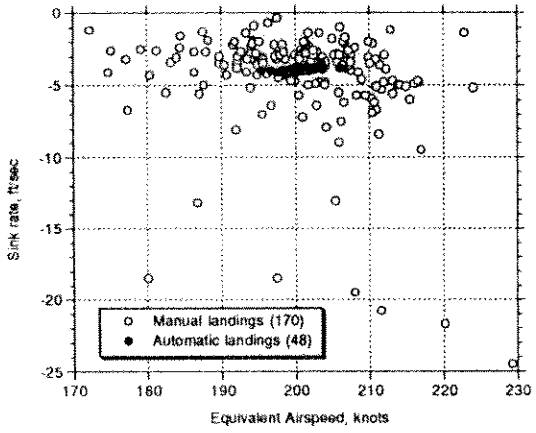

Figure 15. - Touchdown velocities for manual and automatic landings in various wind and turbulence conditions; L/D ~ 4.3

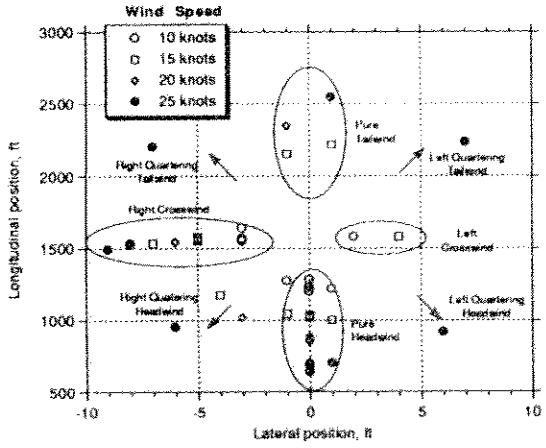

Figure 16. - Autoland touchdown dispersion: 48 landings moderate turbulence, various winds, L/D ~ 4.3

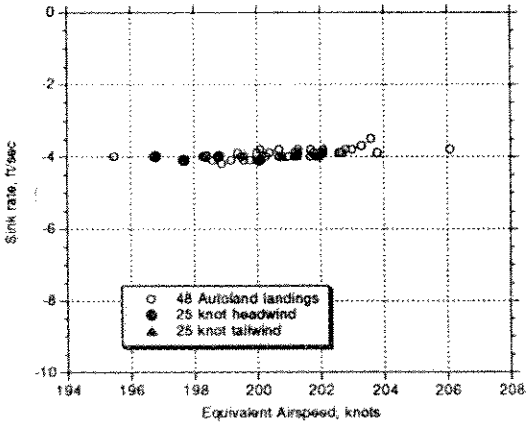

Figure 17. - Autoland touchdown velocities: 48 landings moderate turbulence, various winds, L/D ~ 4.3

they had been made later in the program. In addition, use of a real-time simulator has demonstrated the satisfactory flying and landing characteristics of this type of lifting-body vehicle.

References

[1]Manke, John A.; Retelle, John P.; and Kempel, Robert W.: Assessment of Lifting Body Vehicle Handling Qualities. AIAA Paper No. 71-310, 1971.

[2]Kemple, Robert W.: Flight Evaluation of HL-10 Lifting Body Handling Qualities at Mach Numbers from 0.30 to 1.86. NASA TN D-7537, 1970.

[3]Nagy, Christopher J.; and Kirsten, Paul W.: Handling Qualities and Stability Derivatives of the X-24B Research Aircraft. AFFTC-TR-76-8, 1976.

[4]Smith, Harriet J.: Evaluation of the Lateral-Directional Stability and Control Characteristics of the Lightweight M2-F1 Lifting Body at Low Speeds. NASA TN D-3022, 1965.

[5]Powell, Richard W., Cruz, Christopher I.: Guidance and Control Analysis of the Entry of a Lifting Body Personnel Launch Vehicle, AIAA-91-0055, January 1991

[6]Jackson, E. Bruce and Cruz, Christopher I.: Preliminary Subsonic Aerodynamic Model for Simulation Studies of the HL-20 Lifting Body. NASA TM-4032, 1991

[7]Jackson, E. Bruce; Rivers, Robert A.; and Bailey, Melvin L.: Effect of Lift-to-Drag Ratio Upon Pilot Rating for a Preliminary Version of the HL-20 Lifting Body. AIAA-91-2890, August 1991